

AD-A136 107

PERTURBATIONS ON THE RECEPTION CHARACTERISTICS OF  
ANTENNAS ON DIEGO GARCIA (U) MASSACHUSETTS INST OF TECH  
LEXINGTON LINCOLN LAB R WEBER 28 OCT 83 ETS-71

1/1

UNCLASSIFIED

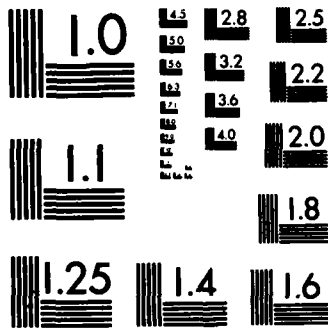
ESD-TR-83-061 F19628-80-C-0002

F/G 9/5

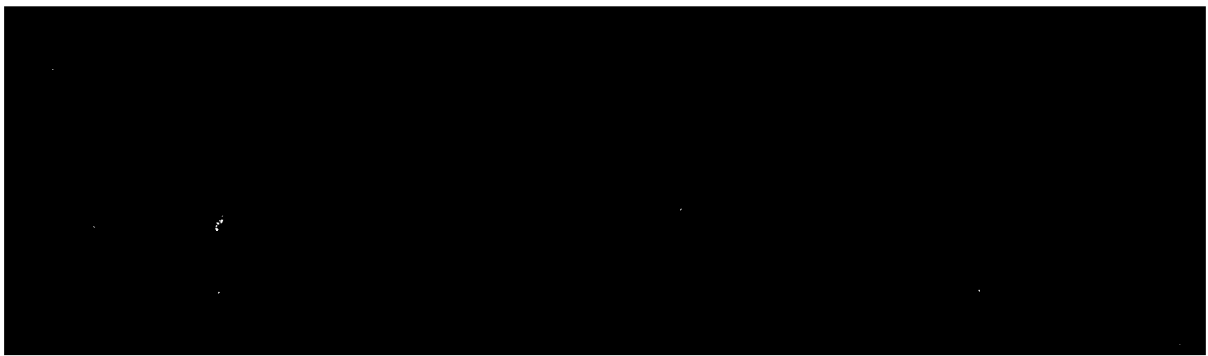
NL

END

FILMED  
104  
ETC



MICROCOPY RESOLUTION TEST CHART  
NATIONAL BUREAU OF STANDARDS-1963-A



**MASSACHUSETTS INSTITUTE OF TECHNOLOGY  
LINCOLN LABORATORY**

**PERTURBATIONS ON THE  
RECEPTION CHARACTERISTICS OF ANTENNAS  
ON DIEGO GARCIA DUE TO THE PRESENCE  
OF A GEODSS SITE**

*R. WEBER*

*Group 94*

**PROJECT REPORT ETS-71**

**28 OCTOBER 1983**

**Approved for public release; distribution unlimited.**

**LEXINGTON**

**MASSACHUSETTS**

### Abstract

The U. S. Navy has developed a large part of Diego Garcia into a support facility. As a consequence, many receiving antennas have been installed. The search for possible locations for a GEODSS site on the northern part of the island (the most developed part) resulted in the consideration of available areas in and near the receiving antenna field. A natural concern was the possible degradation of the reception characteristics of antennas adjacent to the GEODSS structures in each of the selected areas. This report describes in detail the techniques used to determine that degradation when the GEODSS site is directly in the antenna field. Since the method is general, only the results are presented for two additional cases. For all cases, the conclusion is that for well-designed receiving systems, the degradation due to the GEODSS buildings would be negligible.

<b>Accession For</b>	
NTIS GRA&I	<input checked="" type="checkbox"/>
DTIC TAB	<input type="checkbox"/>
Unannounced	<input type="checkbox"/>
Justification _____	
By _____	
Distribution/ _____	
<b>Availability Codes</b>	
<b>Dist</b>	Avail and/or Special
A-1	



## CONTENTS

Abstract	iii
Figures and Table	v
I. INTRODUCTION	1
II. CASE 1. A SITE IN THE RECEIVING ANTENNA FIELD	2
A. Location	2
B. Worst-Case Site Configuration	2
III. COMPUTER ANALYSIS AND RESULTS	8
IV. CONSLUSIONS FOR CASE 1.	17
V. RESULTS AND CONCLUSIONS FOR CASES 2 AND 3.	18
Acknowledgements	21

## Figures

1. Map of Diego Garcia	3
2. Map showing the receiver area on Diego Garcia	4
3. Worst-case site configuration	6
4. Characteristics of the inverted cone antenna	9
5. Perturbations at 2 mHz for the ideal ground case	10
6. Perturbations at 30 mHz for the ideal ground case	11
7. Ground reflection coefficient at 2 mHz	13
8. Ground reflection coefficient at 30 mHz	14
9. Radiation patterns for ideal and real ground cases, 2 mHz	15
10. Radiation patterns for ideal and real ground cases, 30 mHz	16
11. Map of Diego Garcia for Case 3	19

## Table

I. Characteristics of antennas of interest for case 1	5
---	---

## I. INTRODUCTION

Early in the search for a suitable location for a GEODSS site on Diego Garcia, the question arose as to what would be the impact of such an installation--containing three telescope towers, each with a metal dome--on the reception characteristics of nearby antennas. This report describes the analysis performed to answer that question for three different situations. While the description is given in detail for one case, the results are given for the remaining two cases.

The general question to be answered is: Can a location be found for a GEODSS site in, or adjacent to, the receiving antenna area that will have an acceptably small impact on the reception characteristics (i.e., the frequency--dependent relative sensitivities to received signals as a function of direction) of the neighboring antennas? To answer this question, the following approach was taken. First, based on land availability, the knowledge of the reception patterns of the existing antennas, and the "rule of thumb" of staying about a full wavelength (approximately) away from all antennas, a specific location in the antenna field was selected for a GEODSS site. Then, a worst-case configuration of the site was assumed. Using reciprocity and Maxwell's equation with appropriate boundary conditions, the perturbations on the receiving patterns of neighboring antennas were calculated. In this analysis, ideal ground (unity reflection) was assumed initially in order to arrive at the perturbation values. Then, real ground was considered and the differentials between ideal ground and real ground cases were used to calculate the final pattern perturbations.



## II. CASE 1. A SITE IN THE RECEIVING ANTENNA FIELD

### A. Location

We now consider the location for this case and the worst-case site configuration. Figure 1 is an overview of Diego Garcia. The receiving antenna area is indicated in the upper left-hand corner of the map. Figure 2 shows the antenna field and the first location chosen according to the criteria mentioned earlier. From the center of the vertically polarized inverted cone antenna, H01, to the center of the "GEODSS square" is approximately 900 feet. This is almost two wavelengths at the lowest operating frequency of 2 MHz. As for the rhombics, N02 and N04, the selected location is well out of the main radiation pattern of either antenna, with the shortest distance from the center of the GEODSS square to the rear pole of N04 being approximately 750 feet. Again, this distance exceeds a full wavelength distance at the lowest operating frequency of either unit. The operating frequencies and the azimuthal coverages of the antennas of interest are presented in Table I.

### B. Worst-Case Site Configuration

The worst-case site configuration is shown in the next fig. (3). The telescope towers have been modeled as curtains of vertical, perfect conductors (radiators and reflectors). The vertical height of each curtain is 40 ft. and its width is 32 ft. Clearly, this tower model is much more severe than the real structure (largely non-metallic) in terms of producing perturbations to the radiation patterns of nearby antennas. The placement and form of the curtains suggest that the perturbations to the rhombic patterns are entirely negligible. Preliminary investigations showed this to be true.

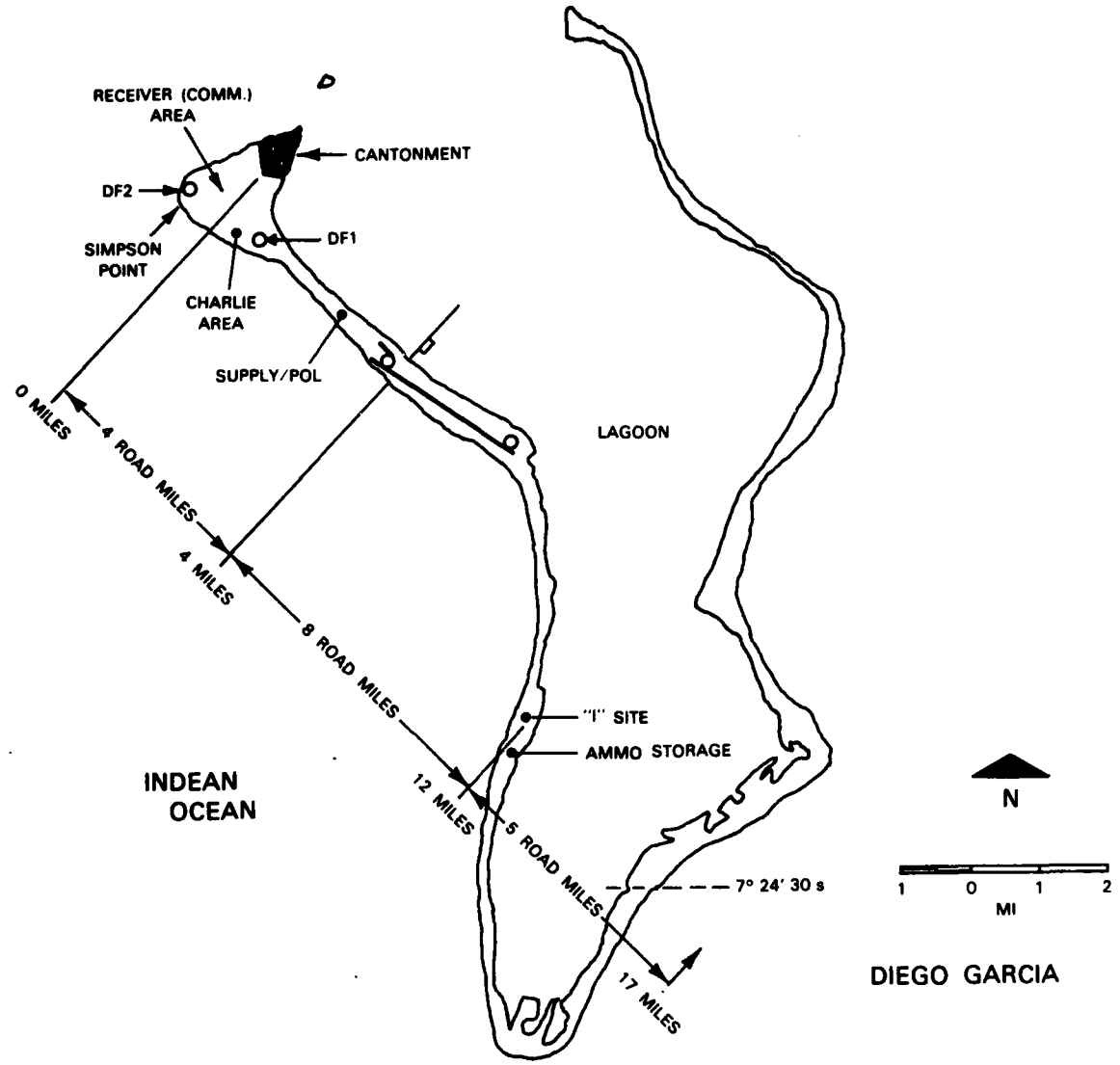


Fig. 1. Map of Diego Garcia showing the location of the receiver area and the two direction-finder locations (labelled "DF").

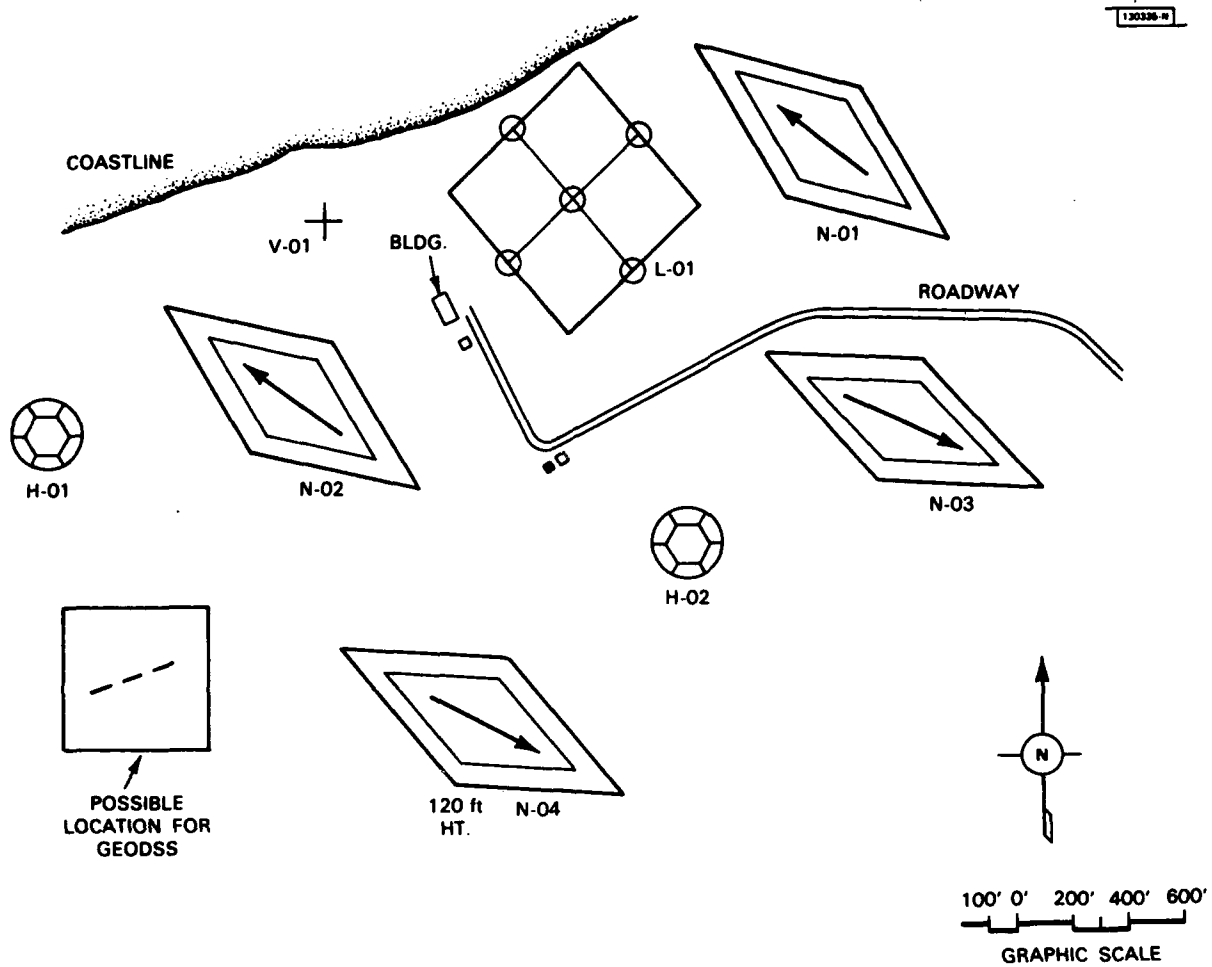


Fig. 2. The receiver area on Diego Garcia showing the proposed location for a GEODSS site. The antenna of primary concern is the vertically polarized inverted cone, H-01.

TABLE I

THE OPERATING FREQUENCIES AND AZIMUTHAL COVERAGES OF THE ANTENNAS OF IMMEDIATE INTEREST IN THE RECEIVER AREA (SEE FIG. 2)

H.F. RECEIVING ANTENNA				
NO.	TYPE	DESCRIPTION	FREQ (MHZ)	COVERAGE
H-01	GRANGER 794	INVERTED CONE	2-30	F
N-02	LUNAR COMM	NESTED RHOMBIC	4-24	304.3° AZ TRUE
N-04	LUNAR COMM	NESTED RHOMBIC	4-24	115.3° AZ TRUE

130336 N

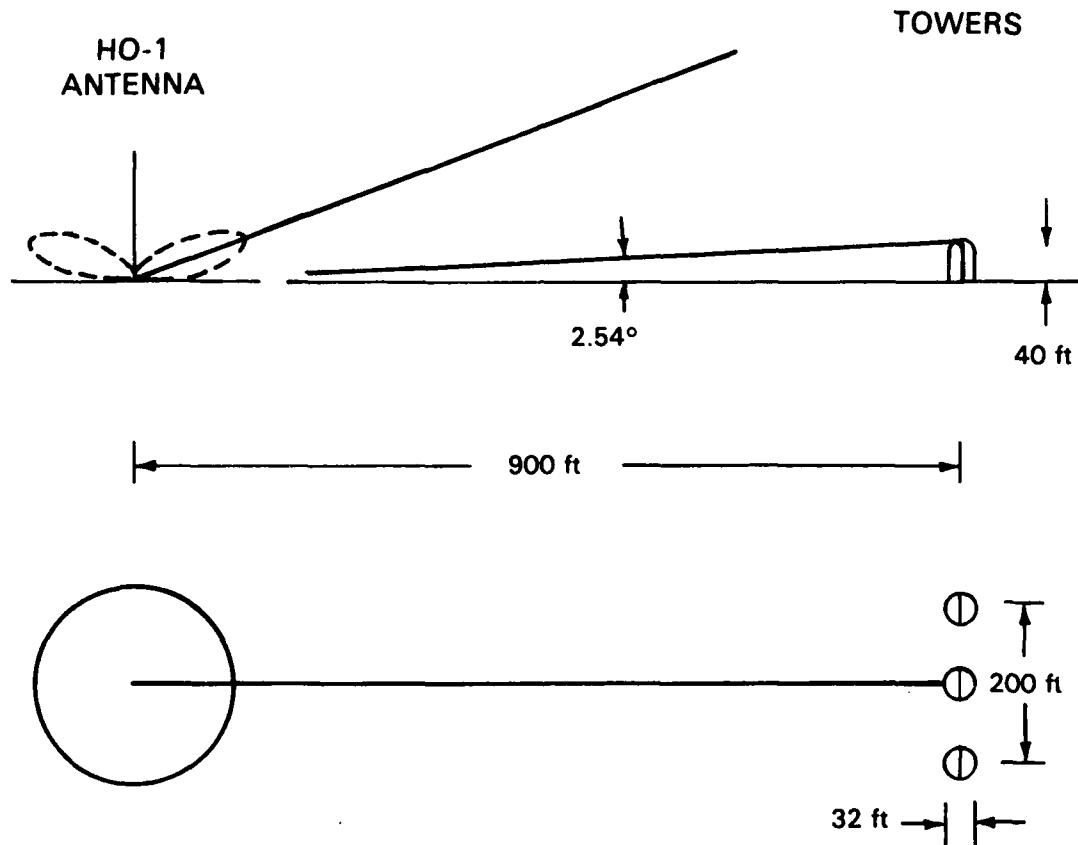


Fig. 3. The worst-case configuration of a GEODSS site. The telescope towers have been replaced by curtains of vertical, perfect conductors.

It is not a surprising result when the radiation angles and the polarizations of the rhombics, and the location of the proposed GEODSS site with respect to the rhombic structures, are considered. As a consequence of this realization, only perturbations to the reception pattern of the inverted cone, H01, will be discussed in the remainder of this report.

### III. COMPUTER ANALYSIS AND RESULTS

At the present time, there exists at Lincoln Laboratory a computer program that treats the problem at hand in as much detail as desired. This perturbation program is highly interactive, requiring for its operation a person with knowledge, skill, and experience in antenna theory. Dr. Andre Dion, a person possessing the required qualities, of Lincoln's Antenna Group, formatted the present problem and supplied the graphs that are to be presented. With this capability available, perturbations for other locations may be quickly determined.

To simplify the input to the perturbation program, and purely as a matter of convenience, the inverted cone was replaced by a vertical dipole. This substitution is justified since the azimuthal patterns are the same in each case and the patterns are the same in elevation up to the peak-gain elevation of each antenna. At this point, it is useful to recall the types of patterns we are dealing with for both ideal and real ground as a function of frequency. Figure 4 shows the published characteristics for the vertically polarized inverted cone antenna. It can be seen from these patterns that under unit ground (ideal) reflection, the patterns have maximum gain toward the flat metal curtains, producing maximum pattern perturbation. The effect of an imperfect (real) ground is to reduce sensitivity of the antenna toward the curtains and to increase the elevation angle of the beam, thereby reducing the perturbations on the pattern.

Computer results for the ideal ground case are shown in Figs. 5 and 6 for frequencies of 2 and 30 MHz. At 2 MHz the perturbation of the pattern of antenna H01 is  $\pm 0.1$  dB. At 30 MHz, it is  $\pm 1.5$  dB. In the latter case,

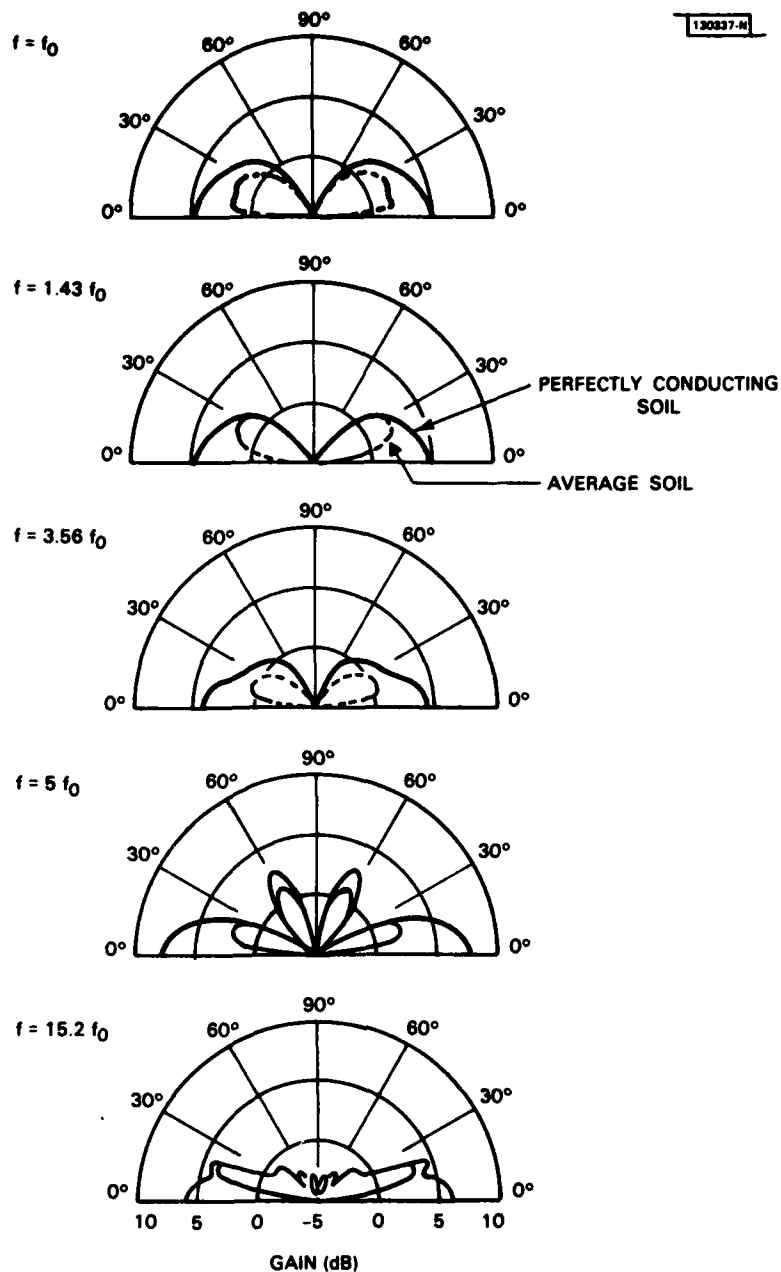


Fig. 4. Published characteristics for the vertically polarized inverted cone antenna. It is observed that the effect of imperfect (real) ground is to reduce the antenna's sensitivity and to increase the elevation angle of the beam, thereby reducing the perturbations caused by nearby structures (e.g., GEODSS towers).



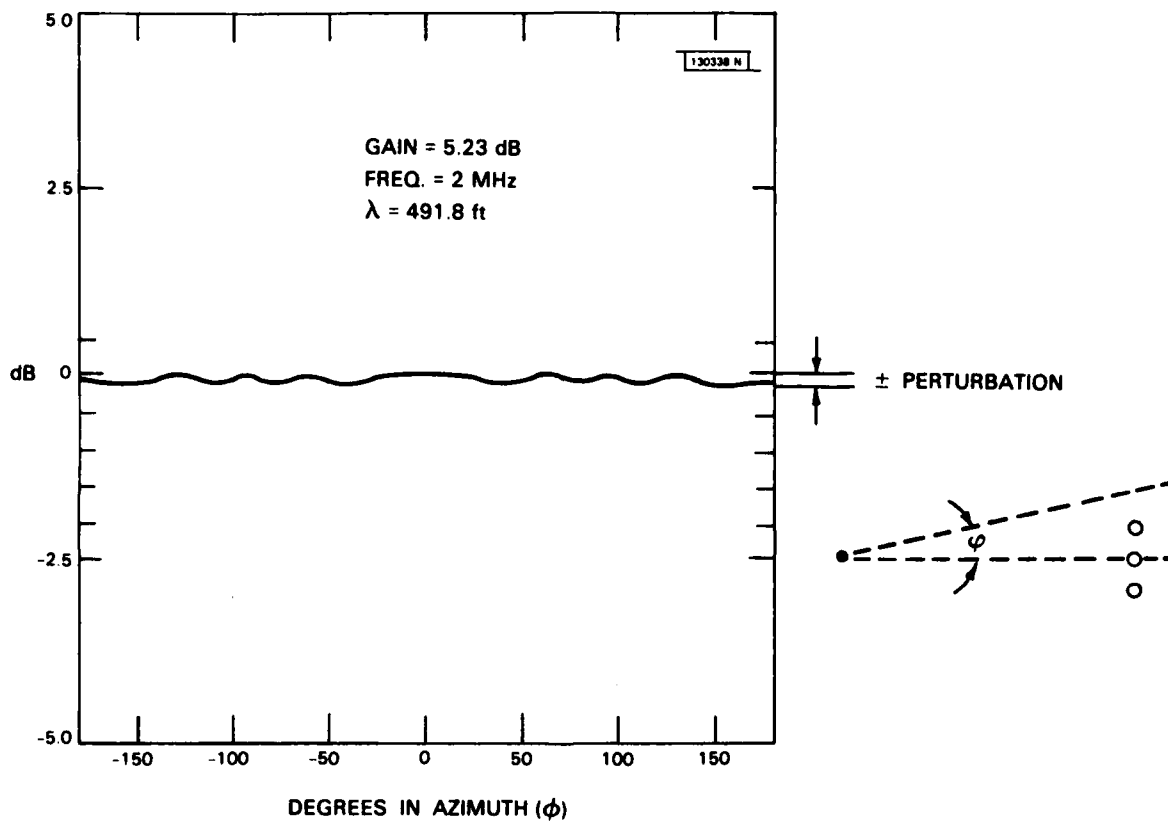


Fig. 5. Computer results for perturbations of 2 mHz for the ideal ground case. The perturbation on the pattern of H-01 is  $\pm 0.1$  dB.

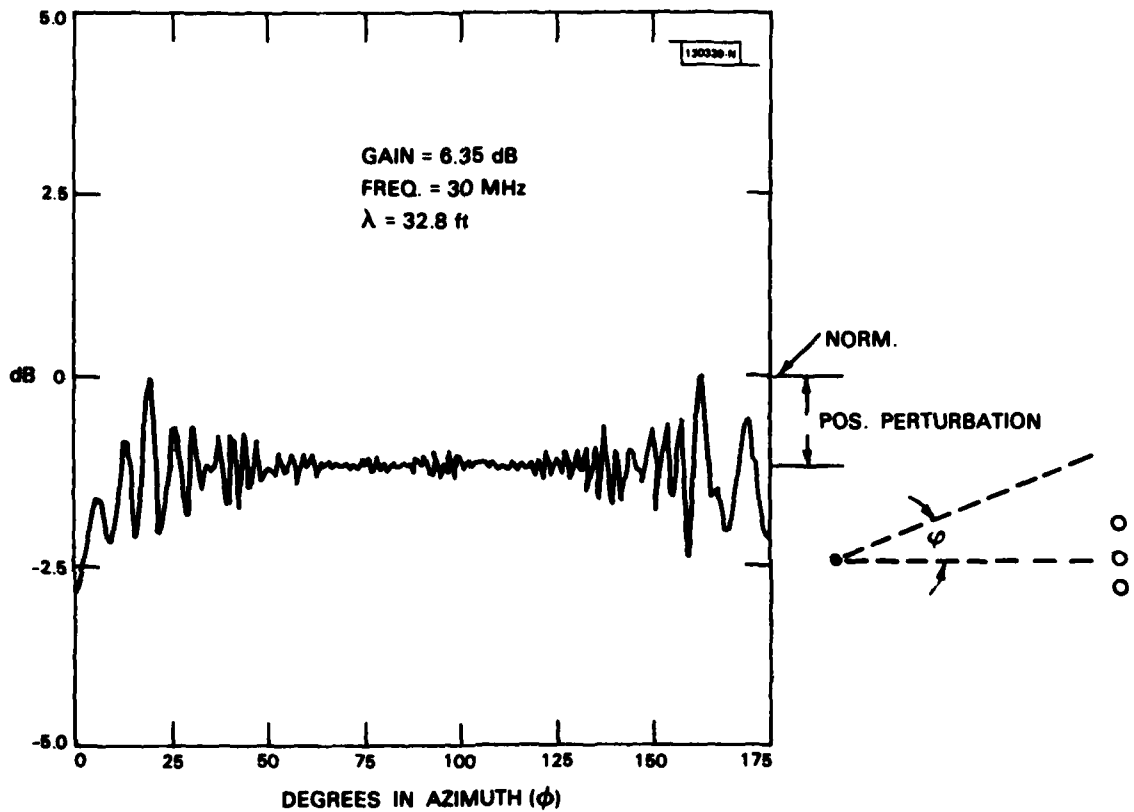


Fig. 6. Computer results for perturbations at 30 mHz for the ideal ground case. The perturbation on the pattern of antenna H-01 is  $\pm 1.5$  dB, the maximum for 2-30 mHz.

the peak disturbance occurs in the vertical plane passing through the center of the curtain configuration and the antenna. The perturbations observed at intermediate frequencies for which the wires of the curtain are resonant were found to be less than the perturbation observed at 30 MHz. Incidentally, it was found that 13 or 14 equally-spaced wires per curtain were sufficient to maximize the perturbations.

In the case of real ground, the effect of low elevation angles is to cause the reflected ray to be out of phase with the direct ray, reducing the antenna gain. For good ground (conductivity,  $\sigma$ , equal to  $5 \times 10^{-3}$  mhos/m and relative dielectric constant,  $k$ , equal to 15), the ground reflection coefficients, as a function of grazing angle for 2 MHz and for 30 MHz, are shown in the next two figs. (7 and 8). The program yields both polarizations, however, only vertical polarization is of interest here.

Next, the radiation patterns of the vertical monopole for these values of ground reflection were computed and are presented in figs. 9 and 10 for 2 and 30 MHz. Here, the ideal-ground and real-ground cases are compared. As can be seen, the gain reductions for both frequencies at an elevation angle of 2.5 degrees, determined by the geometry, are 14 dB at 2 MHz and 18 dB at 30 MHz. The pattern perturbations are correspondingly smaller. At 2 MHz, the "ideal" perturbation was  $\pm 0.1$  dB. With the reduction of 14 dB, it is entirely negligible. At 30 MHz, the "ideal" perturbation was  $\pm 1.5$  dB. The perturbation field in this case is  $\pm 0.19$  of that radiated. This field is now reduced by a factor of 0.126. The resulting pattern perturbation is  $\pm 0.21$  dB.

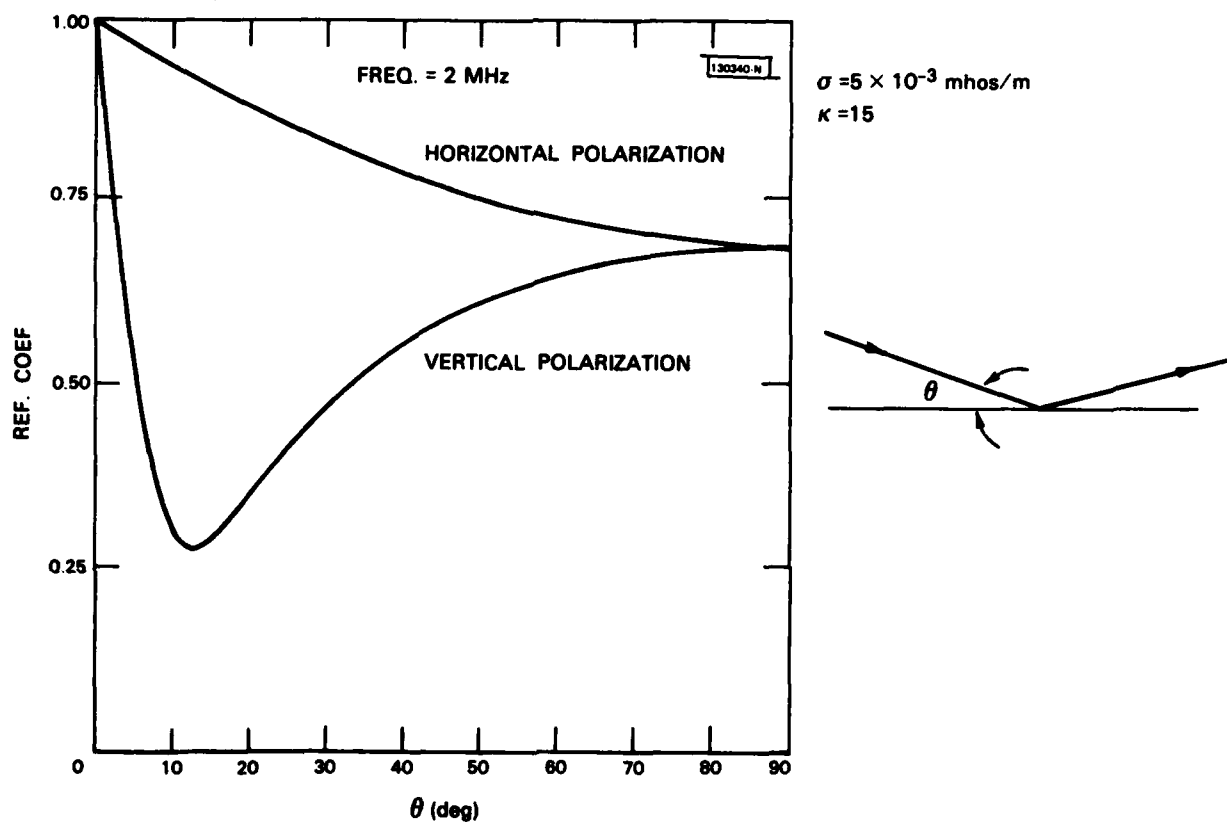


Fig. 7. The ground reflection coefficient as a function of grazing angle,  $\theta$ , for 2 MHz. The vertical polarization result is pertinent in this analysis.

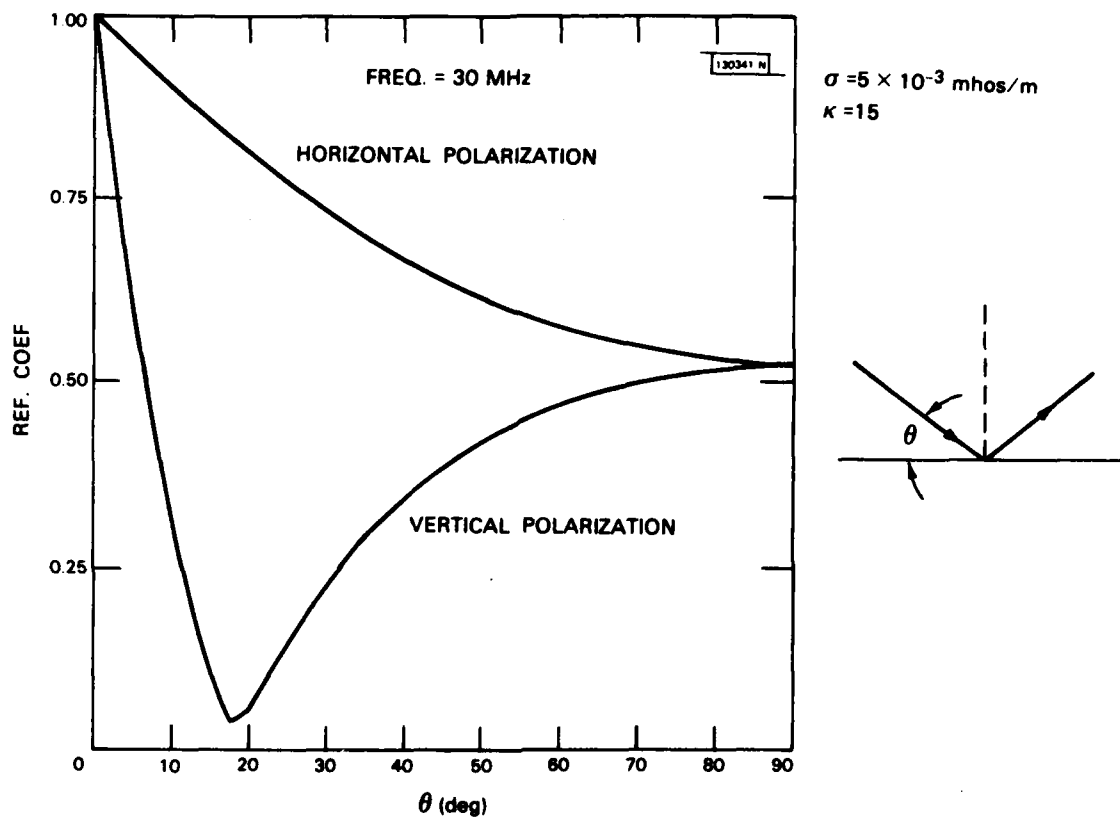


Fig. 8. The ground reflection coefficient as a function of grazing angle,  $\theta$ , for 30 MHz. The vertical polarization case is relevant to this analysis.

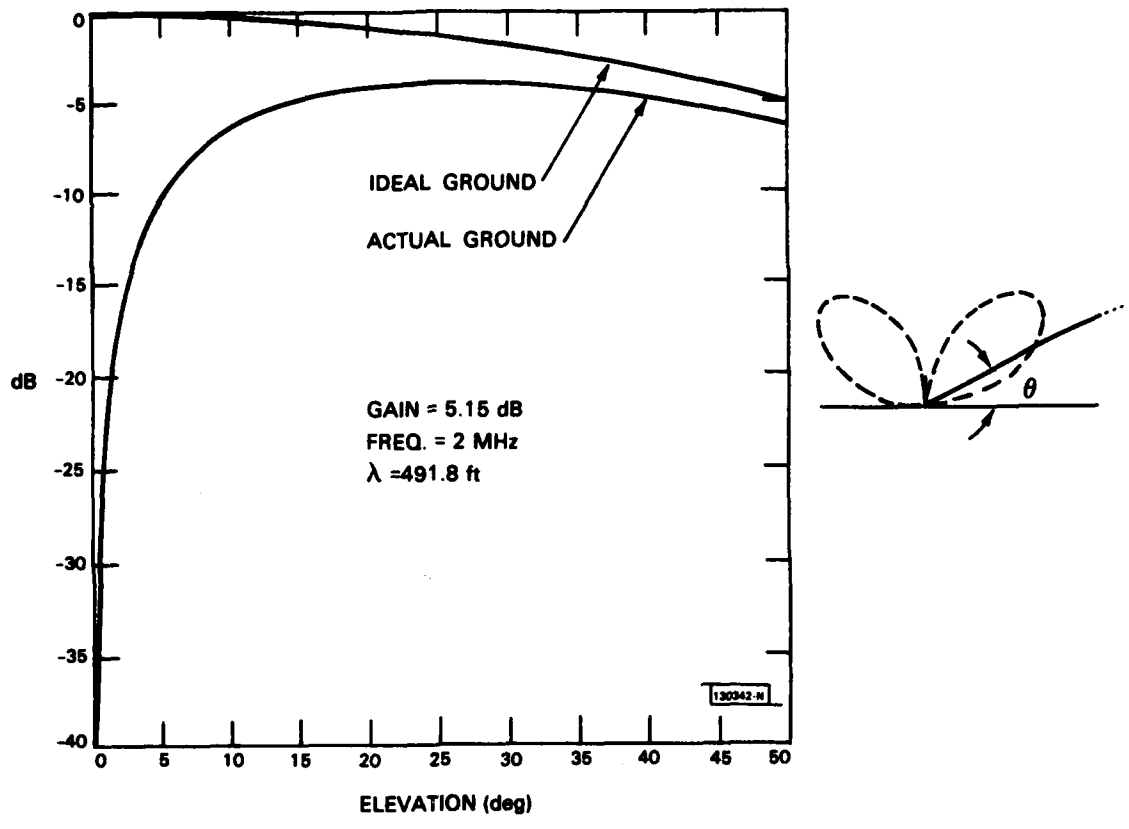


Fig. 9. Radiation patterns of H-01 for the real and ideal ground cases for 2 mHz. At an elevation angle,  $\theta$ , of 2.5 degrees, the gain reduction is 14 dB.

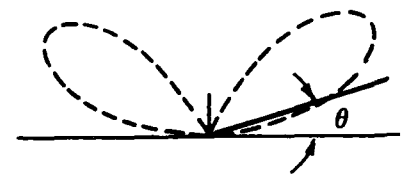
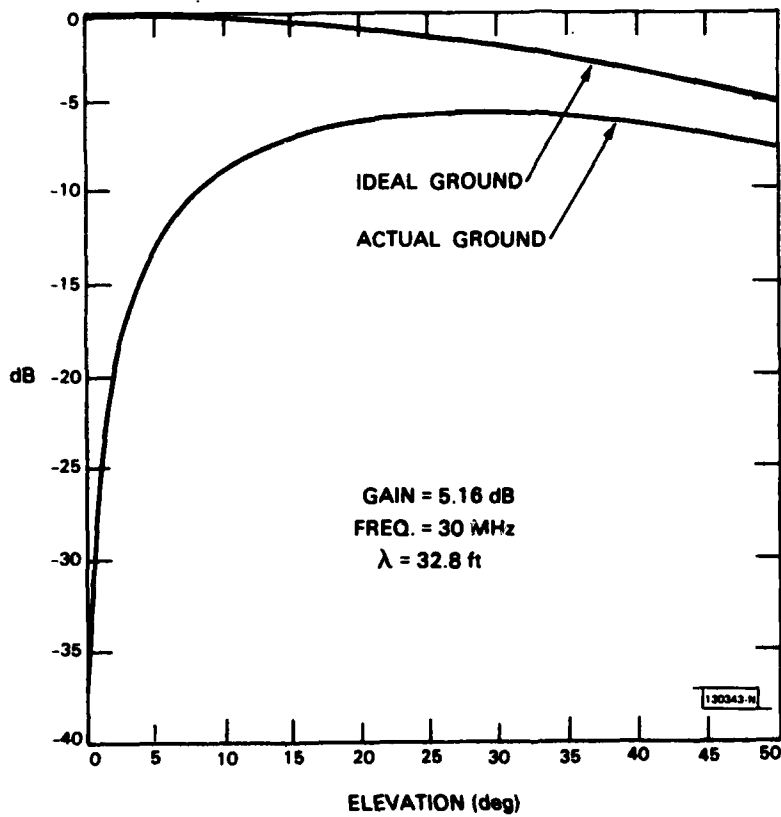


Fig. 10. Radiation patterns of H-01 for the real and ideal ground cases for 30 MHz. At an elevation angle,  $\theta$ , of 2.5 degrees, the gain reduction is 18 dB.

#### IV. CONCLUSIONS FOR CASE 1.

For "good", real ground, and under worst-case conditions--the three telescope towers assumed to be 32' x 40' flat metal surfaces--the maximum pattern perturbation is approximately  $\pm 0.2$  dB over the operating frequency range of the nearby, vertically polarized, inverted cone antenna.

Since the actual telescope buildings will not be metal curtains, but will be concrete structures containing less metal, and since other alignments of the three towers with respect to the inverted cone antenna will be less active in producing perturbations than the configuration used in this analysis, the actual pattern perturbations will be significantly less than the computed and reported value of  $\pm 0.2$  dB. For well-designed receiver systems, this perturbation is negligible.



## V. RESULTS AND CONCLUSIONS FOR CASES 2 AND 3

For these cases, the same general procedure as described for the first case was followed. The worst-case configuration for the GEODSS buildings was the same. Once again, it was determined that arrays of vertically polarized dipole antennas could satisfactorily represent the electrical behaviors of the relevant receiving antennas.

Case 2 considered the perturbations on a direction-finder antenna, if located at the location marked DF2, on Simpson Point (see Fig. 1), due to a GEODSS installation in the receiving field (Case 1). The worst-case results indicated that in the direction of the GEODSS site, the effective range of the antenna would be reduced by 10 percent. Again, the real structure would be responsible for a smaller loss of range.

The final case treated was the configuration in which the GEODSS site is located at the present DF1 location. The antennas of concern are those of the Classic Wizard system (see Fig. 11). Antenna A, the closet unit, is considered here. From antenna A, the GEODSS' tower would subtend an angle of 0.8 degrees; Charlie building subtends an angle of 1.7 degrees. In addition, Charlie building is in the near-field of antenna A; the GEODSS site would be in the far-field. On these bases alone, further analyses were not really required; since, if the presence of Charlie building is operationally acceptable, certainly the addition of the GEODSS site would be no factor at all. Nevertheless, a calculation was performed assuming the absence of Charlie building.

The starting assumption of the analysis was that the antenna would not be pointed to elevations of less than a beamwidth ( $\approx 2^\circ$ ); otherwise, the ground would strongly perturb the pattern. Using reasonable physical and electrical

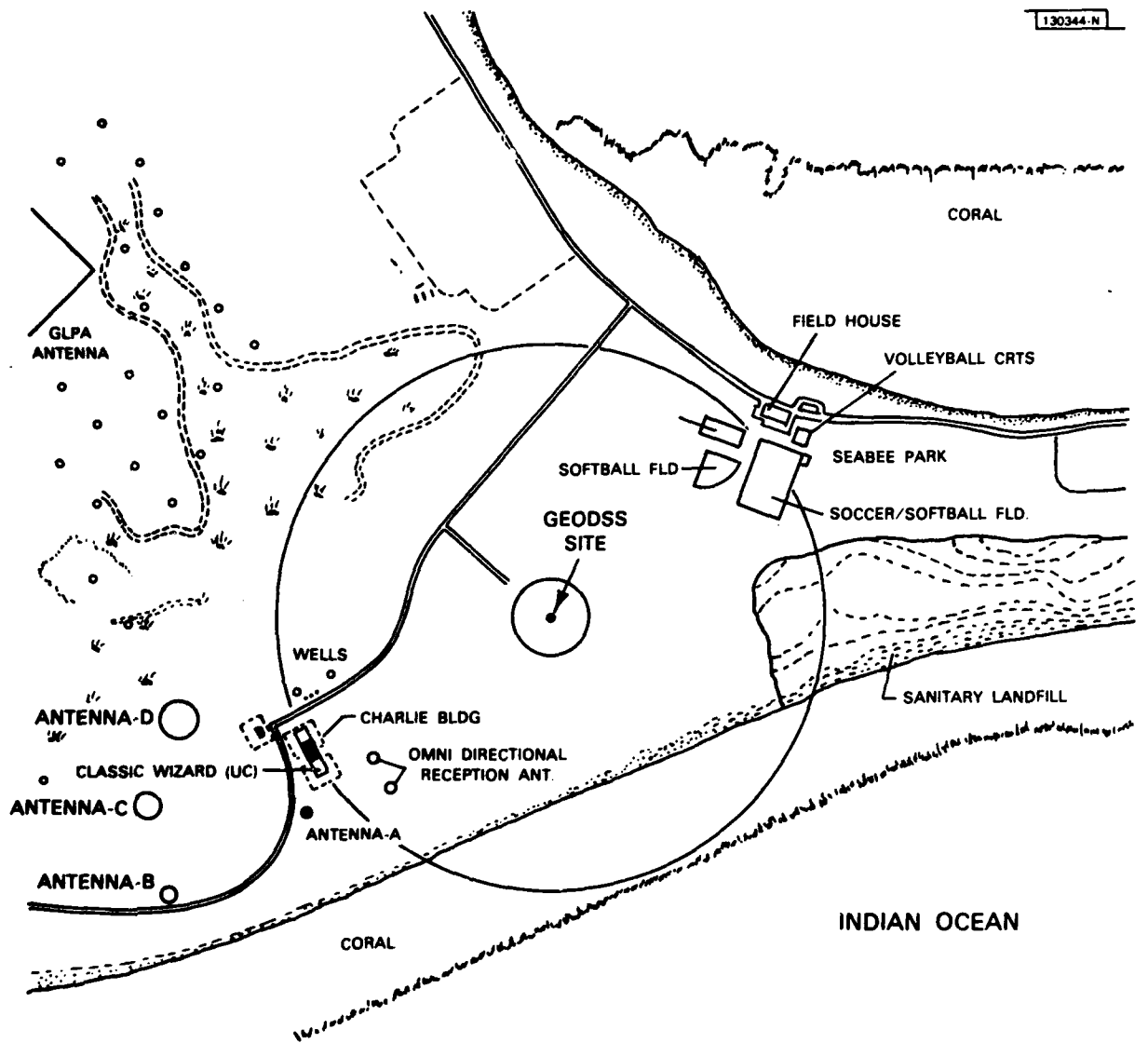


Fig. 11. Map for the third case treated in which the GEOSS site is imagined to be located at DF1 (See Fig. 1). The antennas of interest are those marked A, B, C, and D, elements of the Classic Wizard System.

parameters for antennas of this type, the analysis indicated that while there is no calculable perturbation to the azimuthal pattern, there is some asymmetry introduced into the elevation pattern as the ground is approached from the center of the "beam". The segment of the pattern within  $\pm 0.5$  degrees is virtually unperturbed. As the pointing elevation is increased from 2 degrees, the perturbation decreases, becoming nil at 4 degrees.

The conclusions are that with Charlie building situated as it is, the GEODSS building would not be a factor. Without Charlie building, the GEODSS building would not be a factor for pointing elevations of greater than 4 degrees. For an elevation of 2 degrees, the worst-case GEODSS perturbations will be less of a factor than the local terrain, with or without the GEODSS site at the present DF1 location.

### Acknowledgements

The important contributions of Dr. Andre Dion, of Lincoln's Antenna Group, are appreciated. In addition, I wish to acknowledge his good-humored patience in the face of many questions.

The expert typing of the manuscript by Mrs. Lynne Perry also deserves a word of praise.



**END**

**FILMED**

**1-84**

**DTIC**